

Research Article

Coordination Chemistry of Polyaromatic Thiosemicarbazones 2: Synthesis and Biological Activity of Zinc, Cobalt, and Copper Complexes of 1-(Naphthalene-2-yl)ethanone Thiosemicarbazone

Marc-Andre LeBlanc,¹ Antonio Gonzalez-Sarrias,² Floyd A. Beckford,¹
P. Canisius Mbarushimana,¹ and Navindra P. Seeram²

¹ Science Division, Lyon College, Batesville, AR 72501, USA

² Department of Biomedical and Pharmaceutical Sciences, College of Pharmacy, University of Rhode Island, Kingston, RI 02881, USA

Correspondence should be addressed to Floyd A. Beckford, floyd.beckford@lyon.edu

Received 25 September 2011; Revised 11 November 2011; Accepted 27 November 2011

Academic Editor: Rabindranath Mukherjee

Copyright © 2011 Marc-Andre LeBlanc et al. This is an open access article distributed under the Creative Commons Attribution License, which permits unrestricted use, distribution, and reproduction in any medium, provided the original work is properly cited.

A novel thiosemicarbazone from 2-acetonaphthone (represented as acnTSC) has been synthesized and its basic coordination chemistry with zinc(II), cobalt(II), and copper(II) explored. The complexes were characterized by elemental analysis and various spectroscopic techniques and are best formulated as $[M(\text{acnTSC})_2\text{Cl}_2]$ with the metal likely in an octahedral environment. The anticancer activity of the complexes was determined against a panel of human colon cancer cells (HCT-116 and Caco-2). The compounds bind to DNA via an intercalative mode with binding constants of $9.7 \times 10^4 \text{ M}^{-1}$, $1.8 \times 10^5 \text{ M}^{-1}$, and $9.5 \times 10^4 \text{ M}^{-1}$ for the zinc, cobalt, and copper complexes, respectively.

1. Introduction

The synthesis and chemical investigation of thiosemicarbazones and their metal complexes are of considerable interest due to their potential for medicinal applications. These applications are so varied due to the wide variation in the modes of bonding and stereochemistry [1–6]. Thiosemicarbazones' biological interactions relate to their chelating ability of transition metal ions, a consequence of the unique characteristics of mixed hard-soft NS donor atoms.

The exploration of transition metal complexes as chemical nucleases is well documented because of their biologically accessible redox potentials and relatively high nucleobase affinity [7–9]. Copper thiosemicarbazones have been the focus of investigations as metallodrugs for a long period of time [5, 6, 10–13]. Similar to other drugs seeking to arrest the development of cancer, the cellular targets for such copper complexes are not exactly defined and may be variegate. We studied the interaction of our compounds with DNA, as it is certainly a possible target, but compounds are likely to encounter other biomolecules either at or en route to the site

of action. Thus, proteins must also be considered a possible target for interaction.

As the principal extracellular protein of the circulatory system, human serum albumin (HSA) serves as the major transporter of drugs as well as endogenous compounds. It is well understood that the distribution, free concentration, and the metabolism of various drugs can be significantly altered as a result of their binding to HSA [14]. This potential to act as a transport for drugs makes it important to study the interactions of potential drugs with HSA alongside DNA. Knowledge of the interaction mechanisms between both HSA and DNA with transition metal-thiosemicarbazone complexes is crucial to understanding the pharmacodynamics and pharmacokinetics of a drug or drug prospect. In this paper, we report on the results of a study of a novel thiosemicarbazone from 2-acetonaphthone and its zinc, cobalt, and copper complexes (Figure 1).

2. Experimental

Analytical or reagent grade chemicals were used throughout. All chemicals were obtained from Sigma-Aldrich (St. Louis,

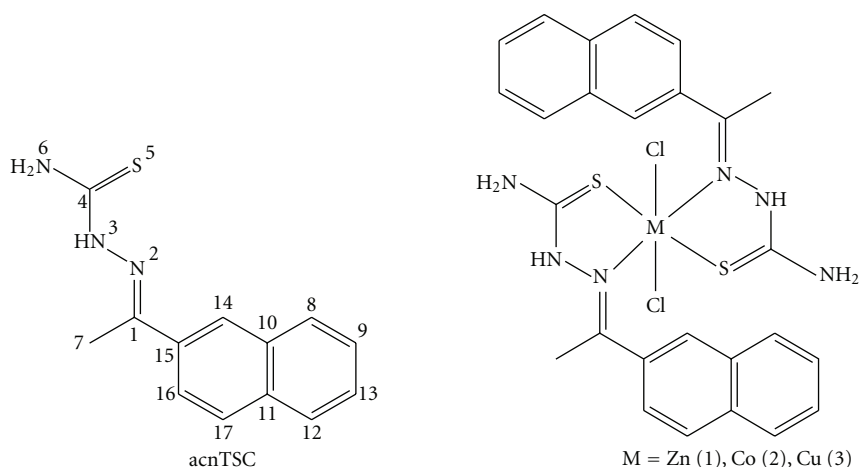


FIGURE 1: Proposed structure of acnTSC and the metal complexes it forms.

MO) or other commercial vendors and used as received. Microanalyses (C, H, N) were performed by Desert Analytics (Tucson, AZ) or Galbraith Laboratories (Knoxville, TN). ^1H and ^{13}C NMR spectra were recorded on Varian Mercury spectrometer operating at 300 MHz in dimethyl sulfoxide- d_6 with the chemical shifts measured in ppm relative to residual protons (2.49) or carbons (39.5). IR spectra were recorded in KBr discs in the range $4000\text{--}450\text{ cm}^{-1}$ on a Nicolet 6700 FTIR spectrophotometer, while the electronic spectra were recorded on an Agilent 8453 spectrophotometer in the range $190\text{--}1100\text{ nm}$ using quartz cuvettes. Fluorescence spectra were recorded on a Varian Cary Eclipse spectrophotometer. Conductivity of 10^{-3} M solutions was measured on a Mettler Toledo SevenMulti conductivity meter. The values reported are averages of triplicate measurements. ESI MS data was acquired on an HP Agilent 1956b single-quadrupole mass spectrometer. Samples were dissolved in methanol, and the solution was introduced by direct injection.

2.1. Synthesis of 2-Acetonaphthone Thiosemicarbazone, acnTSC. Solid 2-acetonaphthone (5.81 g, 0.0342 mol) and thiosemicarbazide (3.17 g, 0.0348 mol) were suspended in 60 mL of absolute ethanol containing a few drops of glacial acetic acid. The mixture was heated at reflux for 5 h, and the white solid that resulted was collected by vacuum filtration, washed with ethanol, and air-dried. Yield 5.45 g (66%). Calculated for $\text{C}_{13}\text{H}_{13}\text{N}_3\text{S}$ C, 64.17; H, 5.39; N, 17.27. Found: C, 63.59; H, 5.01; N, 17.47. ^1H NMR (DMSO- d_6): δ 2.40 (s, H3), 7.50 (m, H6, H7), 7.86 (m, H5, H8), 7.95 (m, H9), 8.28 (d, H10), 8.32 (s, H4), 8.05 and 8.36 (s, H1), 10.29 (s, H2). ^{13}C NMR: δ 13.84 (C7), 124.12 (C16), 126.36, 126.53 (C13, C9), 126.80 (C17), 127.46 (C14), 127.55 (C12), 128.55 (C8), 132.77 (C15), 133.26 (C10), 135.11 (C11), 147.62 (C1), 178.93 (C4). Major IR bands (cm^{-1} , KBr): 3389, 3224, 3144 ($\text{H}_2\text{--N}_6$, H--N_3); 1587 ($\text{C}_1\text{=N}_2$), 1293, 835 ($\text{C}_4\text{=S}_5$).

2.2. Synthesis of the Metal Complexes. The complexes were synthesized according to the following general method. A suspension of the ligand in 30 mL of ethanol was heated to

boiling, and one-half equivalent of the metal salt (MCl_2) dissolved in the minimum amount of ethanol was then added. The reaction mixture was heated at reflux for 2 h during which time the product precipitated from the solution. It was collected by vacuum filtration, washed with a 5–10 mL of ethanol, and dried at the vacuum pump.

$\text{Zn}(\text{acnTSC})_2\text{Cl}_2$ 1. Yellow powder; yield 72%. Calculated for $\text{C}_{26}\text{H}_{26}\text{Cl}_2\text{N}_6\text{S}_2\text{Zn}$ C, 50.13; H, 4.21; N, 13.49. Found C, 50.25; H, 4.14; N, 13.41. ESI MS (+ve ion mode): m/z 584.07 ($[\text{M--Cl--H}]^+$, 100%). Major IR bands (cm^{-1} , KBr): 3426, 3305, 3238 ($\text{H}_2\text{--N}_6$, H--N_3); 1585 ($\text{C}_1\text{=N}_2$), 1292, 813 ($\text{C}_4\text{=S}_5$).

$\text{Co}(\text{acnTSC})_2\text{Cl}_2$ 2. Blue-green powder; yield 82%. Calculated for $\text{C}_{26}\text{H}_{26}\text{Cl}_2\text{CoN}_6\text{S}_2$ C, 50.65; H, 4.25; N, 13.63. Found C, 50.28; H, 4.26; N, 13.51. ESI MS (+ve ion mode): m/z 580.07 ($[\text{M--Cl}]^+$, 100%). Major IR bands (cm^{-1} , KBr): 3426, 3303, 3228 ($\text{H}_2\text{--N}_6$, H--N_3); 1587 ($\text{C}_1\text{=N}_2$), 1290, 813 ($\text{C}_4\text{=S}_5$).

$\text{Cu}(\text{acnTSC})_2\text{Cl}_2$ 3. Yellow powder; yield 67%. Calculated for $\text{C}_{26}\text{H}_{26}\text{Cl}_2\text{CuN}_6\text{S}_2$ C, 50.28; H, 4.22; N, 13.90. Found C, 51.95; H, 4.47; N, 13.53. ESI MS (+ve ion mode): m/z 549.10 ($[\text{M--2Cl}]^+$, 100%). Major IR bands (cm^{-1} , KBr): 3420, 3224, 3133 ($\text{H}_2\text{--N}_6$, H--N_3); 1593 ($\text{C}_1\text{=N}_2$), 815 ($\text{C}_4\text{=S}_5$).

2.3. Bio- and Medicinal Chemistry. The investigations of the reactions of the metal complexes with calf-thymus DNA (ct-DNA) and human serum albumin (HSA) and their cytotoxic evaluation were performed as described previously [15]. The complexes were evaluated against two human colon cancer cells: HCT116 (human colon carcinoma) and Caco-2 (human epithelial colorectal adenocarcinoma). In addition, normal human colon cells, CCD-18Co (human colon fibroblasts), were included.

3. Discussion

3.1. Nuclear Magnetic Resonance. The NMR spectrum of the ligand confirms that, in solution, it exists as the neutral form.

The ligand is very soluble in DMSO, and so the NMR spectrum was obtained in DMSO- d_6 . The ^1H NMR spectrum of the ligand shows typical patterns for a thiosemicarbazone. The N3 hydrogen (Figure 1) resonates as a sharp singlet at 10.29 ppm. The N6 hydrogens generate two distinct singlets at 8.05 and 8.36 ppm. This pattern is to be expected as the protons are magnetically nonequivalent as a consequence of the C4–N3 bond possessing some π character via the mesomeric effect. This results in hindered rotation about this bond which is common in thioamides. The protons of the aromatic moiety show at 7.50–8.32 ppm. The methyl (C7) protons resonate at 2.40 ppm which is typical for a methyl-ketone functional group. The absence of a signal at \sim 4.00 ppm that can be ascribed to —SH [16] is consistent with the idea that in solution, as in the solid state, the ligand exists as the thione tautomer.

The ^{13}C NMR spectrum for the ligand is exactly as would be expected. Of special note is the high frequency signal near 180 ppm which is due to the thioamide carbon, C4. The resonance for the acetyl carbon (C7) occurs at 13.84, and the imine carbon (C1) is seen at 147.62 ppm. The aromatic carbons are observed between 124 ppm and 136 ppm.

3.2. Infrared Spectra. Thiosemicarbazones exhibit characteristic bands corresponding to various functional groups in specific energy regions. Thiosemicarbazone ligands can coordinate in a number of different ways. Most commonly they bind as either of two tautomeric forms—a neutral thione form or the anion from the thiol form. Infrared spectrophotometry can be used to identify the coordinated form, and it was observed that the characteristic absorption peaks of all complexes are similar. The absence of a $\nu(\text{S-H})$ absorption in the region 2600–2500 cm^{-1} is considered as evidence that the thione form of the ligand exists in the solid state [16]. There are three medium bands in the $\nu(\text{N-H})$ region (3450–3150 cm^{-1}), and these signals play an important role in evaluating the nature of the bonding in the complexes. The presence of a band corresponding to N3–H group suggests the coordination of a thiosemicarbazone to the metal center in a neutral form, while its absence would be suggestive of deprotonation of the azomethinic proton in the complexes. The presence of this band supports the thione formulation of the ligand in the complexes, and they do not shift significantly on complexation. On the other hand, for **1** and **2**, there is an unusually large shift in one of the bands associated with N6. The size of the shift is unexpected as this nitrogen is not directly involved in binding. It is apparent that the ligation of the thiocarbonyl sulfur (S5) has led to quite dramatic changes in the electronic current of this functional group.

The coordination sites can also be inferred from the spectral bands attributed to the C1=N2 iminic and C4=S5 thioamide IV groups. The ligand shows a medium intensity band at 1585 cm^{-1} that we ascribe to C=N, and these are shifted slightly to higher or lower energy upon complexation. The involvement of the thiocarbonyl group can similarly be inferred from the wavenumber shifts that occur on binding. The bands in the free ligand attributed to the C=S group shifts to lower frequencies by \sim 20 cm^{-1} . The size

of the shifts suggest that the ligand coordinates as a neutral, bidentate (through N2 and S5) ligand in all the complexes. This is supported by the absence of all the tell-tale signs of thiolate formation particularly the presence of the azomethinic hydrogen in all the complexes.

3.3. Reaction of the Complexes with DNA

3.3.1. Electronic Absorption Spectroscopy. Metal complexes binding to DNA can occur via a variety of mechanisms including intercalation between the base pairs, groove binding, and electrostatic binding. Electronic absorption spectroscopy is a common and effective method to examine the binding interactions (modes and extent) of metal complexes with DNA [17–19]. Given the structure of the complexes under investigation with the flat, extended aromatic moiety, we initially speculated that the compounds should be capable of binding to DNA through intercalation. Complexes which adopt this method of binding generally have electronic absorption bands that are red-shifted relative to the free complex and also display hypochromism. It is accepted that this is due to stacking interactions of the aromatic groups with the DNA base pairs. Absorption titration experiments of **1**, **2**, and **3** in buffer (5 mM Tris, 50 mM NaCl, pH 7.2) were performed by using solutions with a fixed complex concentration (10^{-4} M^{-1}) to which increments of a concentrated solution of ct-DNA were added. The solutions were allowed to stir for 5 minutes after each addition before the absorption spectra were recorded (Figure 2). It can be seen from the figure that as the DNA concentration is increased, there is hypochromism of the main absorption band though no obvious red-shift of the same band was observed.

Consequently, we can suggest that the complexes can indeed intercalate into the DNA structure. The extent of hypochromism is often consistent with the extent of binding, but, to quantify the binding strength, the intrinsic binding constant K_b can be calculated from the following equation [17]:

$$\frac{[\text{DNA}]}{\epsilon_a - \epsilon_f} = \frac{[\text{DNA}]}{\epsilon_b - \epsilon_f} + \frac{1}{K_b(\epsilon_b - \epsilon_f)}, \quad (1)$$

where ϵ_a , ϵ_f , and ϵ_b correspond to the molar absorptivities of the metal complex after each addition of ct-DNA, for the free metal complexes and for the metal complexes in the fully bound form, respectively. From the plots of $[\text{DNA}]/(\epsilon_a - \epsilon_f)$ versus $[\text{DNA}]$ (insets of Figure 2), the binding constants K_b are calculated from the ratio of the slope of the intercept. The values are given in Table 1. From the table, it is seen that the binding constant are on the order of 10^4 – 10^5 M^{-1} which characterizes them as moderately strong intercalators. It was also observed that the cobalt complex (**2**) is significantly stronger as a binder compared to **1** or **3**. Given the close structural similarity between the complexes, we are not sure as to why this might be.

3.3.2. Fluorescence Competition Experiment. To further investigate the binding mode between the complexes and DNA,

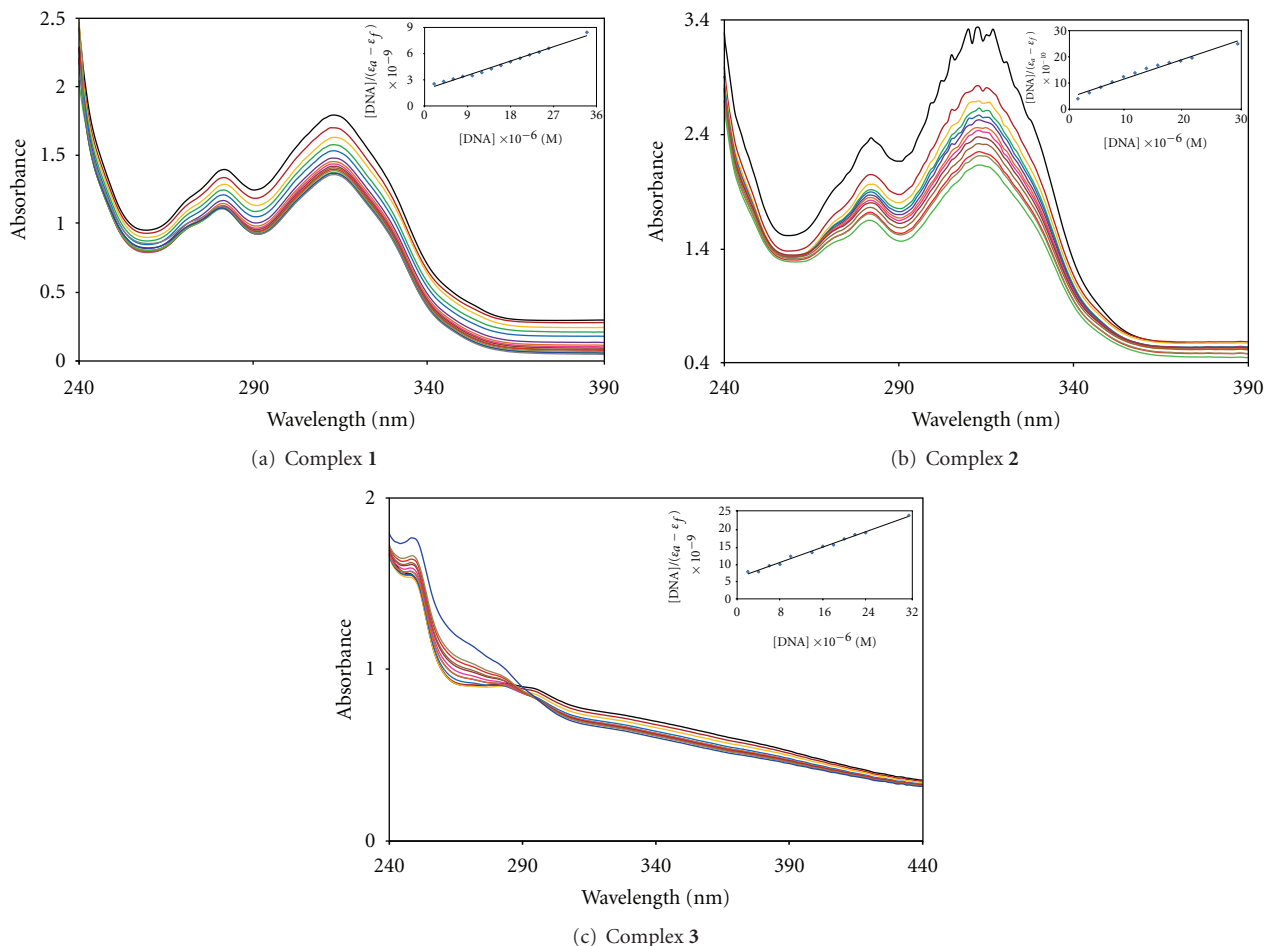


FIGURE 2: Electronic absorption spectral (hypochromic) changes of the complexes on titration with ct-DNA. $[M] = 10 \mu\text{M}$, $[\text{DNA}] = 0-34 \mu\text{M}$. Insets: plot of $[\text{DNA}]/(\epsilon_a - \epsilon_f)$ versus $[\text{DNA}]$.

TABLE 1: Binding constants for the reaction of the complexes with ct-DNA.

Compound	λ (nm)	$10^4 K$ (M^{-1}) (R^2)	% hypochromicity
1	325	9.7 ± 0.6 (0.988)	89
2	312	17.8 ± 0.3 (0.977)	36
3	330*	9.5 ± 0.4 (0.990)	13

* measured at shoulder.

fluorescence competition experiments with ethidium bromide (EB) were employed. EB is a planar cationic dye well known to intercalate into the DNA helix. The EB-DNA adduct is a strong fluorescence emitter on excitation near 520 nm. Quenching of the fluorescence may be used to determine the extent of the binding between the quencher (in this case the complexes) and DNA. As a typical example, consider the reaction with **1** (Figure 3). It is obvious that there is a decrease in the fluorescence at 600 nm as the amount of added **1** is increased. This supports the idea that **1** can interact with DNA by the intercalative mode. The complex **2** also displays this pattern of behavior.

We can also perform a quantitative assessment of the interaction from the EB titration. This may be done by

carrying out a Stern-Volmer analysis of the data. According to the Stern-Volmer equation (2), the relative fluorescence is directly proportional to the concentration of the quencher:

$$\frac{F_0}{F} = 1 + K_{SV}[Q] = 1 + K_q\tau_o[Q]. \quad (2)$$

Here, F_0 and F are the fluorescence intensity of the EB-DNA adduct before and after the addition of the complex, K_{SV} is the Stern-Volmer quenching constant, and $[Q]$ is the concentration of the quencher (in this case the complex). For a homogeneously emitting solution, (1) predicts a linear plot of F_0/F versus $[Q]$ and that is what we observe for the two complexes (**1** and **2**) studied (inset of Figure 3). The values of K_{SV} and K_q can be obtained from (1) since K_{SV} is the ratio of the slope to the intercept. For **1** and **2**, K_{SV} was calculated to be $(7.48 \pm 0.29) \times 10^3 \text{ M}^{-1}$ and $(5.78 \pm 0.19) \times 10^3 \text{ M}^{-1}$, respectively. These values indicate that the complexes are only moderately strong quenchers. The values of K_q are also informative. For the two complexes studied, the calculated values are on the order of $10^{11} \text{ M}^{-1}\text{s}^{-1}$ (using $\tau_o = 22 \text{ ns}$ [20]). The numbers are an order of magnitude larger than the maximum ($10^{10} \text{ M}^{-1}\text{s}^{-1}$ [21]) allowed for aqueous reactions. Consequently, we can suggest that the type of quenching that is occurring in the reactions is predominantly static.

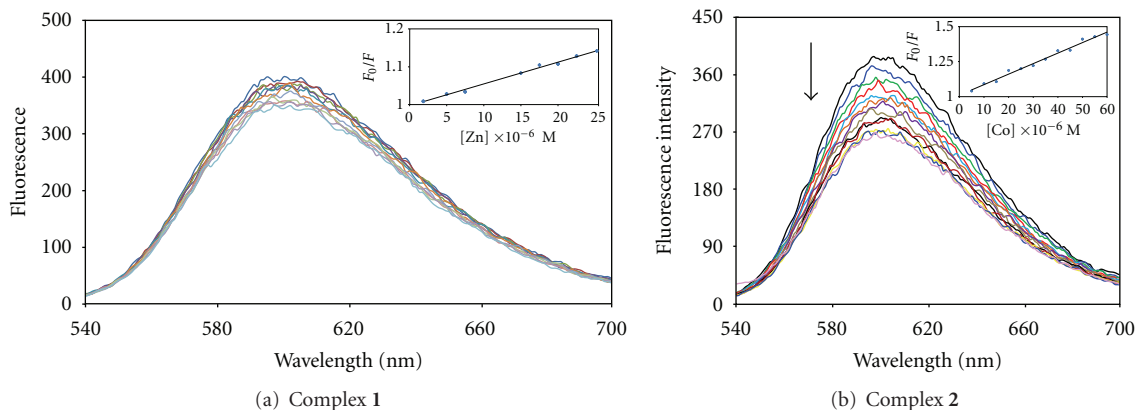


FIGURE 3: Fluorescence spectra of the EB-DNA complex in the absence and presence of increasing amounts of **1** and **2**, $\lambda_{\text{ex}} = 520 \text{ nm}$, $[\text{EB}] = 0.33 \mu\text{M}$, $[\text{DNA}] = 10 \mu\text{M}$, $[\text{complex}] (\mu\text{M})$: 0–60 in $5 \mu\text{M}$ increments. Temperature = 298 K.

The linearity of the Stern-Volmer plot is usually associated with the fluorophore possessing a single binding site or multiple accessible binding sites. Consequently, the apparent binding constant (K_{app}) for **1** with ct-DNA was determined by using (3) [22]:

$$K_{\text{app}} = \frac{K_{\text{EB}}[\text{EB}]}{[\text{complex}]_{50\%}}, \quad (3)$$

where $K_{\text{EB}} = 1.2 \times 10^6 \text{ M}^{-1}$ and the binding constant of EB to DNA and $[\text{complex}]_{50\%}$ is the concentration of **1** at 50% of the initial fluorescence. The binding constants for **1** and **2** are $3.53 \times 10^3 \text{ M}^{-1}$ and $3.98 \times 10^3 \text{ M}^{-1}$. These values indicate a moderate binding affinity that is not typical for a classical intercalator. It may be that the aromatic rings of the thiosemicarbazone moiety do not extend far enough away from the metal center to allow for deep penetration into the DNA helix. The similarity of the binding constants for the two complexes is not unexpected given the similarity in geometry, and there is no apparent effect of the metal center on DNA binding. However, this is not the same result as the observed from the absorption titration experiments.

3.3.3. Viscometric Studies. We have studied the interaction of the complexes with DNA by viscometry. This method is the most definitive way to verify if a small molecule can bind to DNA via an intercalative mechanism. The classical DNA intercalators will lengthen the strands resulting in an increase in the viscosity of the DNA solutions. On the other hand, complexes that bind exclusively in the DNA grooves by a partial or nonclassical intercalation of the compound (under the same conditions) can reduce its effective length and, consequently, its viscosity by bending the DNA helix. The viscometric data, presented as a plot of $(\eta/\eta_0)^{1/3}$ versus the binding ratio $[\text{complex}]/[\text{DNA}]$, is shown in Figure 4. It was observed for the complexes that the viscosity of the DNA solutions did change over the studied range of metal concentrations. There is an increase in the viscosity of the solutions followed by a decrease at higher concentrations (for **1**). This would suggest that the complexes interact with DNA via weak or partial intercalation. Given the

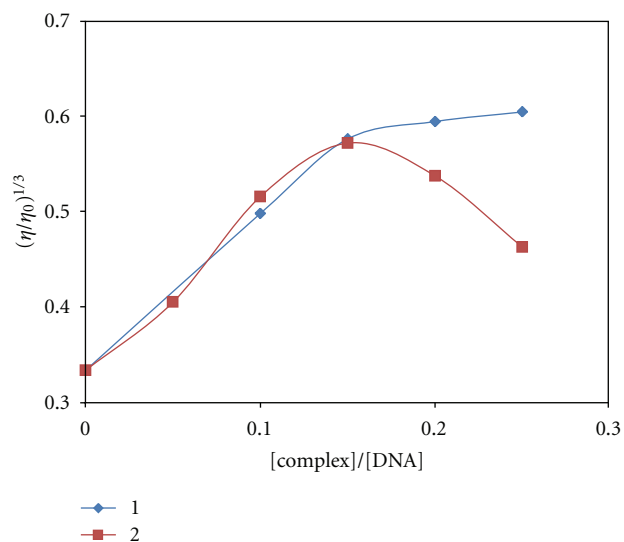


FIGURE 4: Effect of increasing concentrations of complexes **1** and **2** on the relative viscosity of ct-DNA solutions at $304 \text{ K} \pm 1 \text{ K}$.

electronic and structural nature of the thiosemicarbazone substructure, major intercalation into DNA by this moiety seems improbable. So the viscometry results support the idea that if the complexes intercalate into DNA, the interaction is weak.

Chemical Nuclease Activity. The chemical nuclease activity of complexes has been assessed by their ability to convert supercoiled pBR322 DNA from Form I (supercoil) to Form II (open circular) by agarose gel electrophoresis in the dark as well as with UV irradiation under aerobic conditions. When circular plasmid DNA is probed by electrophoresis, relatively fast migration is normally observed for Form I. If scission occurs on one strand (nicking), the supercoil will relax to generate a slower-moving Form II. Figure 5 shows the electrophoretic separation of the DNA after incubation with the complexes in the dark. In general, it is clear that the complexes **2** and **3** show some cleavage of the DNA at

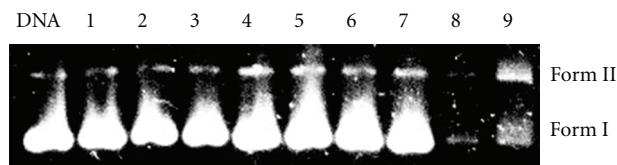


FIGURE 5: Agarose gel electrophoresis diagram for the cleavage of pBR322 DNA by the complexes at ambient temperature in the dark under aerobic conditions. Incubation time was 1 h. Lane DNA, DNA alone; Lane 1, DNA + 10 μM 1; Lane 2, DNA + 50 μM 1; Lane 3, DNA + 100 μM 1; Lane 4, DNA + 10 μM 2; Lane 5, DNA + 50 μM 2; Lane 6, DNA + 100 μM 2; Lane 7, DNA + 10 μM 3; Lane 8, DNA + 50 μM 3; Lane 9, DNA + 100 μM 3.

the three concentrations studied (10, 50, and 100 μM). There are no significant differences in the cleavage ability of the complexes.

3.4. Reaction of the Complexes with HSA. Human serum albumin (HSA) is the most abundant blood serum protein and serves as a transport unit for a wide variety of endogenous substances including drugs. In this study, we investigated the binding of the complexes to HSA using fluorescence spectroscopy. HSA has a well-known structure that contains a single tryptophan residue that is responsible for the majority of the intrinsic fluorescence of the protein. On excitation at 295 nm, HSA has strong fluorescence emission at 350 nm. This emission can be attenuated by a small molecule binding at or near the tryptophan as this amino acid unit is quite susceptible to changes in its environment. As a representative example, Figure 6 shows that addition of **2** to HSA can very efficiently reduce the fluorescence so we can conclude that the complexes in general can bind to HSA. We can obtain a quantitative estimate of the strength of this binding by treating the data with the Stern-Volmer equation (2). Treatment of the data in this manner resulted in the plots shown in the inset of Figure 6. It was observed that the plots were not linear as predicted from the equation but showed significant positive deviations from linearity at higher concentration of added metal complexes.

There are two common explanations for this deviation. First, the HSA fluorescence can be quenched via both of the common quenching mechanisms operating simultaneously. For proteins, the quenching constant is approximately the same [23, 24]. Alternatively, there may be more than one independent binding site on the HSA, and they are not all equivalently accessible to the complexes. Under these circumstances, the binding constant for the reaction can be obtained from a modified Stern-Volmer (MSV) analysis [23]. This involves treating the data using (4):

$$\frac{F_0}{F_0 - F} = \frac{1}{fK[\text{Ru}]} + \frac{1}{f}. \quad (4)$$

Here, f = fraction of the fluorophore that is initially accessible to the complex. This may be interpreted as the number of binding sites on the protein. K is the effective quenching constant for the fluorophore which can be taken

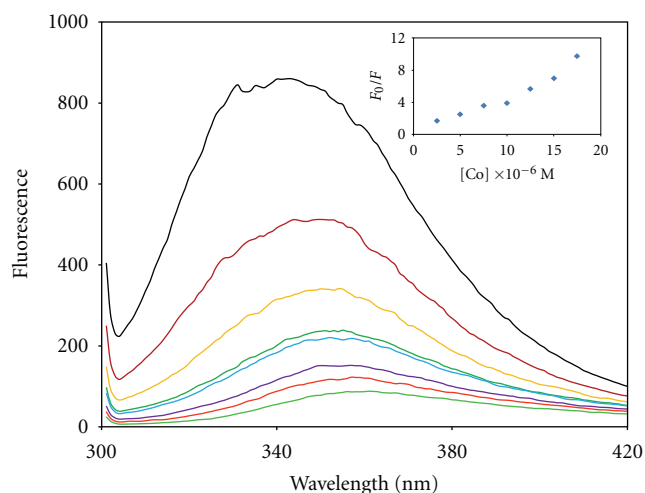


FIGURE 6: Emission spectra of HSA in the absence and presence of increasing amounts of **2**, $\lambda_{\text{ex}} = 295 \text{ nm}$, $[\text{HSA}] = 5.0 \mu\text{M}$ and $[\mathbf{2}]$ (μM): 0–20 in 2.5 μM increments. Temperature = 298 K.

TABLE 2: Binding constants for the interaction of the complexes with HSA (calculated from the modified Stern-Volmer equation).

Temp. (K)	$10^4 K (\text{M}^{-1}) (R^2)$		
	1	2	3
298	8.91 ± 0.49 (0.997)	23.2 ± 0.1 (0.996)	2.67 ± 0.70 (0.995)
308	27.7 ± 1.2 (0.994)	6.14 ± 0.89 (0.989)	1.95 ± 0.20 (0.990)

as a binding constant assuming the decrease in fluorescence comes from the interaction of the HSA with the complexes. Figure 7 shows the plot of $F_0/F_0 - F$ versus $1/[\text{metal}]$ from which we obtain K from the ratio of the intercept to the slope. The derived binding constants are between 10^4 and 10^5 M^{-1} (Table 2) indicating that they are strong binders. For all three compounds, the average number of binding sites as measured by f was determined to be about 1.4. This number does not conclusively settle the question as to whether there is a single binding site on the protein.

3.5. Cytotoxicity Assay. The *in vitro* cytotoxicity of the complexes **1–3** against two human cancer cell lines, HCT-116 (colon carcinoma) and Caco-2 (epithelial colorectal adenocarcinoma), and a noncancerous cell line, CCD-18Co (colon fibroblasts), was investigated using a tetrazolium-based (MTS) colorimetric assay. Etoposide, a potent antineoplastic drug, was used as a standard comparison treatment. The IC_{50} values (Table 3), the median cytotoxic concentrations, were determined after 24, 48, and 72 h of drug exposure. Generally, the longer the exposure time, the more cytotoxic the complexes with the 72 h exposure time being as much as three times more effective compared to the 24 h exposure. As another generality, the Caco-2 cell line is slightly more sensitive to the complexes than the HCT-116 cell line. For instance, at 72 h exposure, **1** is two times as cytotoxic against the Caco-2 line. It is clear from the table that the copper

TABLE 3: IC₅₀ values (μM) representing the antiproliferative activity of all the complexes in a panel of three human cell lines—2 tumorigenic (HCT-116 and Caco-2) and one noncancerous (CCD-18Co).

Complex	HCT-116			Caco-2			CCD-18Co		
	24 h	48 h	72 h	24 h	48 h	72 h	24 h	48 h	72 h
1	20.6 ± 2.6	13.7 ± 2.3	10.8 ± 1.4	15.6 ± 2.1	8.5 ± 2.4	5.4 ± 0.4	16.3 ± 3.0	7.5 ± 0.7	5.0 ± 1.5
2	60.7 ± 2.5	20.4 ± 4.8	8.5 ± 0.5	56.3 ± 3.3	15.2 ± 3.2	5.6 ± 0.7	59.4 ± 1.6	16.2 ± 1.9	7.8 ± 1.0
3	3.7 ± 0.8	2.6 ± 0.5	1.5 ± 0.5	3.0 ± 0.1	1.5 ± 0.7	1.0 ± 0.1	2.8 ± 0.3	1.7 ± 0.2	1.1 ± 0.2
Etoposide	29.6 ± 1.7	23.3 ± 1.1	19.3 ± 1.5	21.8 ± 2.2	15.3 ± 0.9	14.0 ± 1.3	48.4 ± 1.2	43.7 ± 1.7	40.3 ± 2.0

Each assay was carried out utilizing the MTS method following a 24-, 48- or 72-hour drug-incubation period at 37°C. IC₅₀ values are means ± standard deviations (of three replicate measurements).

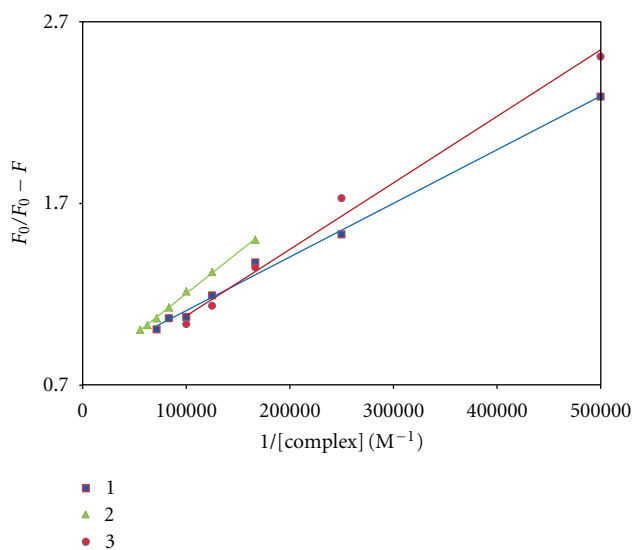


FIGURE 7: Plot of the modified Stern-Volmer equation: $F_0/(F_0 - F)$ versus $1/[Ru]$, for the reaction of the complexes with HSA.

complex (3) is the most active complex we studied with excellent activity against both cancer cell lines. For the 72 h exposure, the IC₅₀ values are near 1 μM which is ten times as active as the zinc complex (1) and five times as active as the cobalt complex (2) for the HCT-116 cell line. Compound 3 is even more active, under our assay conditions, than the etoposide drug comparison. Unfortunately, we have also seen that the complexes are not anymore active against the two cancer cell lines versus the noncancerous cell line.

Considering the cytotoxicity of the complexes in relation to the DNA binding, it seems as if the anticancer activity of the complexes is not comprehensively related to the interaction with DNA; the complex with the lowest *in vitro* activity has the highest DNA binding constant.

Acknowledgments

The project described was supported by Award no. P20RR16460 from the National Center for Research Resources to FAB. The authors are very grateful for the help of Professor Alvin Holder and Mr. Joshua Philips at the University of Southern Mississippi (Hattiesburg, MS, USA) in obtaining the mass spectrometric data. The content is solely

the responsibility of the authors and does not necessarily represent official views of the National Centre for Research Resources or the National Institutes of Health.

References

- [1] E. Hess and G. Bahr, "Über emprotide Schwermetall-Innerkomplexe der α-Diketondithiosemicarbazone (Thiazone). I," *Zeitschrift für Anorganische und Allgemeine Chemie*, vol. 268, no. 4–6, pp. 351–363, 1952.
- [2] G. Bähr, E. Hess, E. Steinkopf, and G. Schleitner, "Über emprotide Schwermetall-Innerkomplexe der α-Diketondithiosemicarbazone (Thiazone). II," *Zeitschrift für Anorganische und Allgemeine Chemie*, vol. 273, no. 6, pp. 325–332, 1953.
- [3] G. Bahr and E. Schleitner, "Über emprotide Schwermetall-Innerkomplexe der α-Diketondithiosemicarbazone (Thiazone). III," *Zeitschrift für Anorganische und Allgemeine Chemie*, vol. 278, no. 3–4, pp. 136–154, 1955.
- [4] C. J. Jones and J. A. McCleverty, "Complexes of transition metals with Schiff bases and the factors influencing their redox properties—part I: nickel and copper complexes of some diketone bis-thiosemicarbazones," *Journal of the Chemical Society A*, pp. 2829–2836, 1970.
- [5] D. H. Petering, *Carcinostatic Copper Complexes*, Marcel Dekker, New York, NY, USA, 1980, Edited by H. Sigel.
- [6] D. X. West, I. H. Hall, K. G. Rajendran, and A. E. Liberta, "The cytotoxicity of heterocyclic thiosemicarbazones and their metal complexes on human and murine tissue culture cells," *Anti-Cancer Drugs*, vol. 4, no. 2, pp. 231–240, 1993.
- [7] V. Brabec and O. Nováková, "DNA binding mode of ruthenium complexes and relationship to tumor cell toxicity," *Drug Resistance Updates*, vol. 9, no. 3, pp. 111–122, 2006.
- [8] K. Li, L. H. Zhou, J. Zhang et al., "Self-activating" chemical nuclease: ferrocenyl cyclen Cu(II) complexes act as efficient DNA cleavage reagents in the absence of reductant," *European Journal of Medicinal Chemistry*, vol. 44, no. 4, pp. 1768–1772, 2009.
- [9] B. Maity, M. Roy, and A. R. Chakravarty, "Ferrocene-conjugated copper(II) dipyrrophenazine complex as a multifunctional model nuclease showing DNA cleavage in red light," *Journal of Organometallic Chemistry*, vol. 693, no. 8–9, pp. 1395–1399, 2008.
- [10] I. C. Mendes, J. P. Moreira, A. S. Mangrich, S. P. Balena, B. L. Rodrigues, and H. Beraldo, "Coordination to copper(II) strongly enhances the *in vitro* antimicrobial activity of pyridine-derived N(4)-tolyl thiosemicarbazones," *Polyhedron*, vol. 26, no. 13, pp. 3263–3270, 2007.
- [11] M. B. Ferrari, F. Bisceglie, G. Pelosi et al., "Synthesis, characterization and X-ray structures of new antiproliferative

- and proapoptotic natural aldehyde thiosemicarbazones and their nickel(II) and copper(II) complexes,” *Journal of Inorganic Biochemistry*, vol. 90, no. 3-4, pp. 113–126, 2002.
- [12] D. X. West, J. S. Ives, J. Krejci et al., “Copper(II) complexes of 2-benzoylpyridine ⁴N-substituted thiosemicarbazones,” *Polyhedron*, vol. 14, no. 15-16, pp. 2189–2200, 1995.
- [13] S. Jayasree and K. K. Aravindakshan, “Structural and anti-tumour studies of metal complexes with thiosemicarbazones of β -diketoesters,” *Polyhedron*, vol. 12, no. 10, pp. 1187–1192, 1993.
- [14] U. Krach-Hansen, V. T. G. Chuang, and M. Otagiri, “Practical aspects of the ligand-binding and enzymatic properties of human serum albumin,” *Biological and Pharmaceutical Bulletin*, vol. 25, no. 6, pp. 695–704, 2002.
- [15] F. A. Beckford, J. Thessing, M. Shaloski Jr. et al., “Synthesis and characterization of mixed-ligand diimine-piperonal thiosemicarbazone complexes of ruthenium(II): biophysical investigations and biological evaluation as anticancer and antibacterial agents,” *Journal of Molecular Structure*, vol. 992, no. 1–3, pp. 39–47, 2011.
- [16] M. M. Mostafa, A. El-Hamid, M. Shallaby, and A. A. El-Asmy, “Copper(II), cobalt(II), nickel(II) and mercury(II) complexes of 1,4-diphenylthiosemicarbazide,” *Transition Metal Chemistry*, vol. 6, no. 5, pp. 303–305, 1981.
- [17] A. Ambroise and B. G. Maiya, “Ruthenium(II) complexes of redox-related, modified dipyrrophenazine ligands: synthesis, characterization, and DNA interaction,” *Inorganic Chemistry*, vol. 39, no. 19, pp. 4256–4263, 2000.
- [18] M. Jiang, Y. T. Li, Z. Y. Wu, Z. Q. Liu, and C. W. Yan, “Synthesis, crystal structure, cytotoxic activities and DNA-binding properties of new binuclear copper(II) complexes bridged by N,N'-bis(N-hydroxyethylaminoethyl)oxamide,” *Journal of Inorganic Biochemistry*, vol. 103, no. 5, pp. 833–844, 2009.
- [19] Q. Liu, J. Zhang, M. Q. Wang et al., “Synthesis, DNA binding and cleavage activity of macrocyclic polyamines bearing mono- or bis-acridine moieties,” *European Journal of Medicinal Chemistry*, vol. 45, no. 11, pp. 5302–5308, 2010.
- [20] K. S. Ghosh, B. K. Sahoo, D. Jana, and S. Dasgupta, “Studies on the interaction of copper complexes of (–)-epicatechin gallate and (–)-epigallocatechin gallate with calf thymus DNA,” *Journal of Inorganic Biochemistry*, vol. 102, no. 9, pp. 1711–1718, 2008.
- [21] J. R. Lacowicz, *Principles of Fluorescence Spectroscopy*, Springer, New York, NY, USA, 3rd edition, 2006.
- [22] J. P. Peberdy, J. Malina, S. Khalid, M. J. Haman, and A. Rodger, “Influence of surface shape on DNA binding of bimetallo helicates,” *The Journal of Inorganic Biochemistry*, vol. 101, no. 11-12, pp. 1937–1945, 2007.
- [23] M. R. Eftink and C. A. Ghiron, “Fluorescence quenching of indole and model micelle systems,” *Journal of Physical Chemistry*, vol. 80, no. 5, pp. 486–493, 1976.
- [24] M. R. Eftink and C. A. Ghiron, “Fluorescence quenching studies with proteins,” *Analytical Biochemistry*, vol. 114, no. 2, pp. 199–227, 1981.



Hindawi

Submit your manuscripts at
<http://www.hindawi.com>

